Effects of mutation at a conserved *N*-glycosylation site in the bovine retinal cyclic nucleotide-gated ion channel

Seong-hwan Rho[a], Han Mi Lee[a], Kyunglim Lee[b], Chul-Seung Park[a],*

[a]*Department of Life Science, Kwangju Institute of Science and Technology (K-JIST), Kwangju 500-712, South Korea*
[b]*College of Pharmacy, Ewha Womans University, Seoul 120-750, South Korea*

Abstract Bovine retinal cyclic nucleotide-gated (CNG) ion channel contains an evolutionary conserved *N*-glycosylation site in the external loop between the fifth transmembrane segment and the pore-forming region. The effect of tunicamycin treatment and the site-specific mutation suggested that the channel is glycosylated when expressed in *Xenopus* oocytes. To test the role of glycosylation in this channel, *N*-glycosylation was abolished by mutation, and the detailed permeation and the gating characteristics of the mutant channel were investigated. The charge contribution turned out to be detectable, although the mutation of the *N*-glycosylation site did not affect expression and functionality of the CNG channel in oocytes. © 2000 Federation of European Biochemical Societies. Published by Elsevier Science B.V. All rights reserved.

Key words: *N*-glycosylation; Cyclic nucleotide-gated ion channel; Guanosine 3′,5′-cyclic mononucleotide; Divalent cation blockade; *Xenopus* oocyte

1. Introduction

Cyclic nucleotide-gated channels (or CNG channels) are cation-selective ion channels that open in response to the direct binding of intracellular cyclic nucleotides such as guanosine 3′,5′-cyclic mononucleotide (cGMP) or cAMP. These channels play critical roles in sensory signaling of vertebrate photoreceptors and olfactory neurons [1]. Serving as downstream targets of the signaling pathways, CNG channels mediate the transduction of sensory stimuli into neuronal activity. Related channels have been found in several other tissues including the pineal gland, kidney, heart, and brain [2–5], strongly suggesting that CNG channels may be involved in other important physiological processes in different tissues [6]. CNG channels have several regions homologous to voltage-gated K^+ channels such as the S4 domain and the pore-forming region (P-region) and are also believed to share a similar folding pattern in the membrane. More than one subunit has been identified and the functional CNG channels are thought to be a tetramer of these subunits [7–9].

The α subunit of the bovine retinal CNG channel protein has a putative *N*-glycosylation site that is highly conserved throughout evolution (Fig. 1A). Many recent studies revealed that glycosylation of ion channel proteins dynamically affects some channel functions at the molecular level such as ligand binding, transport activity, gating and stabilization of the open state [10–13], as well as general functions like protein folding, sorting and surface membrane targeting [14–17]. However, the role of *N*-glycosylation in the CNG channel is not known yet. Since the putative glycosylation site is located at the outer vestibule of the CNG channel near the P-region, it may be important structurally and/or functionally [18]. One possibility is that since sialic acid residues of the glycosyl moiety are negatively charged at physiological pH, a cloud of negative charges close to the outer vestibule may change the electrostatic energy profiles and alter the ion permeation [12].

In the present study, we made a mutation replacing Asn-327 to Ser (N327S) of bovine retinal CNGC α subunit to determine whether the Asn-327 residue of the CNG channel is glycosylated in vivo, and to test the effects of the glycosylation on expression and functions of CNG channels in *Xenopus* oocytes. We found that treatment of the wild type channel protein with tunicamycin caused the same shift in the molecular weight of the expressed channel as the N327S mutation and that the unglycosylated form of the CNG channel is still functionally intact.

The effect of the N327S mutation on the permeation and gating characteristics was further investigated in detail at the macroscopic current level using patch clamp techniques. We found that the activation of the N327S mutant by intracellular cyclic GMP and the selectivity for monovalent cations under the bi-ionic conditions were not significantly altered. To study possible surface charge effects of sugar moieties, we evaluated the effects of deglycosylation on the prominent voltage-dependent Mg^{2+} blockade of the CNG channel current [19,20]. A significant difference in the electrical distances (δ) of the extracellular Mg^{2+} binding sites between the wild type and the N327S channel was found, and a charge screening effect by the elevated concentration of extracellular Mg^{2+} was also observed. These results can be explained by the surface charge contribution of glycosylation.

2. Materials and methods

2.1. Mutagenesis and expression
Female *Xenopus laevis* were purchased from Xenopus One (Ann Arbor, MI, USA). Restriction enzymes were purchased from New England Biolabs (Beverly, MA, USA) and Boehringer Mannheim (Mannheim, Germany). T7 RNA Polymerase was purchased from Promega (Madison, WI, USA). Collagenase was from Worthington Biochemical (Freehold, NJ, USA). The cGMP and other chemicals

*Corresponding author. Fax: (82)-62-970 2484.
E-mail: cspark@kjist.ac.kr

were purchased from either Sigma (St. Louis, MO, USA) or Aldrich Chemical Co., Inc. (Milwaukee, WI, USA). Bovine retinal CNG channel α subunit was obtained from Dr. Siegelbaum at the University of Columbia who re-cloned the gene based on the sequence originally determined by Dr. Kaupp's group. The Asn-327 residue of CNG channel α subunit gene was mutated to serine by site-directed mutagenesis using PCR. The wild type and the mutant channel were subcloned into pGH vector without the T7-tag sequence for control and into pRSET vector (Invitrogen Inc.), which has the T7 antibody epitope for expression and electrophysiological study. The total length of the bovine retinal CNG channel α subunit gene with the T7-tag is 2174 nucleotides and this encodes the channel protein of 83 kDa.

2.2. Expression of channel protein in Xenopus oocytes for Western blot analysis and electrophysiological analysis

Complementary RNA of both wild type and N327S construct were prepared by in vitro transcription and about 50 ng of cRNA was microinjected into defolliculated X. laevis oocytes. Oocytes were incubated in ND-96 (96 mM NaCl, 2 mM KCl, 1.8 mM CaCl₂, 1 mM MgCl₂, and 5 mM HEPES, pH 7.6, supplemented with 10 μg/ml gentamicin). Some of them were incubated in ND-96 with 10 μg/ml tunicamycin. After 2–6 days, oocytes were suspended in lysis buffer (100 mM Tris–HCl, 100 mM NaCl, 0.5% v/v Triton X-100, 0.1 mM PMSF at pH 8.0). The homogenate was centrifuged at 14 000 rpm in an Eppendorf microfuge for 5 min. The soluble fraction was subjected to sodium dodecyl sulfate–polyacrylamide gel electrophoresis (SDS–PAGE). Channel proteins with T7-tag were detected by using anti-T7 mouse monoclonal antibody (Novagen, Inc.) and anti-mouse IgG goat antibody conjugated with peroxidase (Upstate, Inc.).

2.3. Electrophyisiological study and data acquisition for patch clamp recordings

Ionic current through the CNG channel was measured by the GΩ sealed membrane patch-clamp method in excised inside-out and outside-out configurations. Patch pipettes were fabricated from borosilicate glass (TW150F-4, World Precision Instruments, Inc.) using a Flaming/Brown micropipette puller (Model P-87, Sutter Instrument Co.). Pipettes were fire-polished with a microforge (MF-83, Narishige Scientific Instrument Lab.) to give the pipette resistance of 3–5 MΩ. The current–voltage (I–V) relationship of the channel's macroscopic current was determined in symmetrical divalent-free buffering environment (130 mM NaCl, 3 mM HEPES, 0.5 mM EDTA at pH 7.6) with 0.5 mM of intracellular cGMP. Each current trace shown is the average of five trials measured with the ramp voltage stimulus from -100 mV to 100 mV over 1 s and a holding voltage of 0 mV. Rapid and complete solution changes were obtained by moving a linear array of microcapillary tubes (1 μl, 64 mm length; Drummond, Inc.), each containing different concentrations of cGMP or Mg^{2+} sequentially.

To investigate the selectivity of both the wild type and the mutant CNG channel, we analyzed the I–V relationship under symmetrical bi-ionic conditions. In the test solutions, 130 mM Na^+ was substituted with the same concentration of other monovalent cations, K^+, Li^+, Rb^+, or Cs^+. In order to prevent non-symmetrical and anomalous mol fraction effects, Na_2–EDTA was replaced by EDTA (free acid) (Sigma E-6758). All the test ions are the hydroxylated forms, which remain symmetric to both intracellular and extracellular solutions after pH adjustment to pH 7.6 with HCl. (KOH, Sigma P-5958; LiOH·H₂O, Sigma L-4256; RbOH, Aldrich Chem CO. 24,389-2; CsOH, Aldrich Chem CO. 23,204-1). For Mg^{2+} blocking experiments, MgCl₂ was added to give the desired free concentration calculated by Martell and Smith [21]. The calculation also took the pH into account. Intracellular cGMP and Mg^{2+} titrations were done in the inside-out patch configuration and extracellular Mg^{2+} titration was done in the outside-out patch configuration. Voltage stimuli were delivered and channel currents were measured using the Axopatch 200B with CV202BU headstage. The analog data were digitized by Digidata 1200B at 12 kHz and filtered at 1 kHz by a 4-pole Bessel filter. The collected data were analyzed by the program: pClamp v.6.0 (Axon Instruments, Inc.) and Origin 4.1 (Microcal, Inc.)
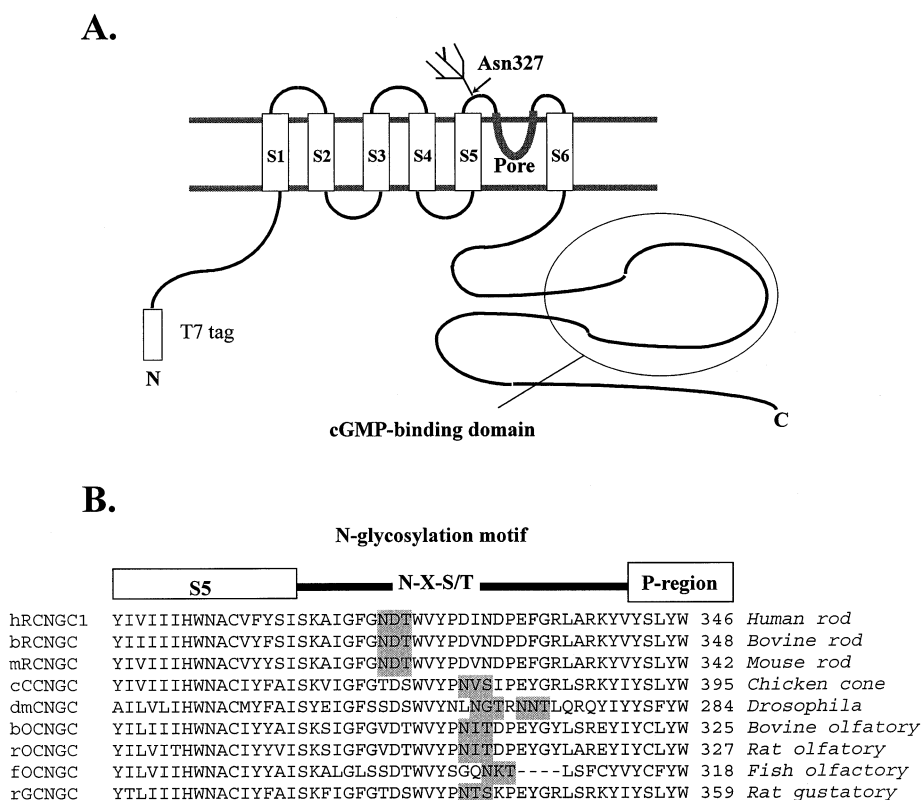

Fig. 1. N-glycosylation of Asn-327 of the wild type and the N327S CNG channels expressed in Xenopus oocytes. A: The putative membrane topology of CNG channel protein. B: The location of a conserved N-glycosylation motif, Asn–X–Ser or Thr (shaded), in various subtypes of the CNG channel.
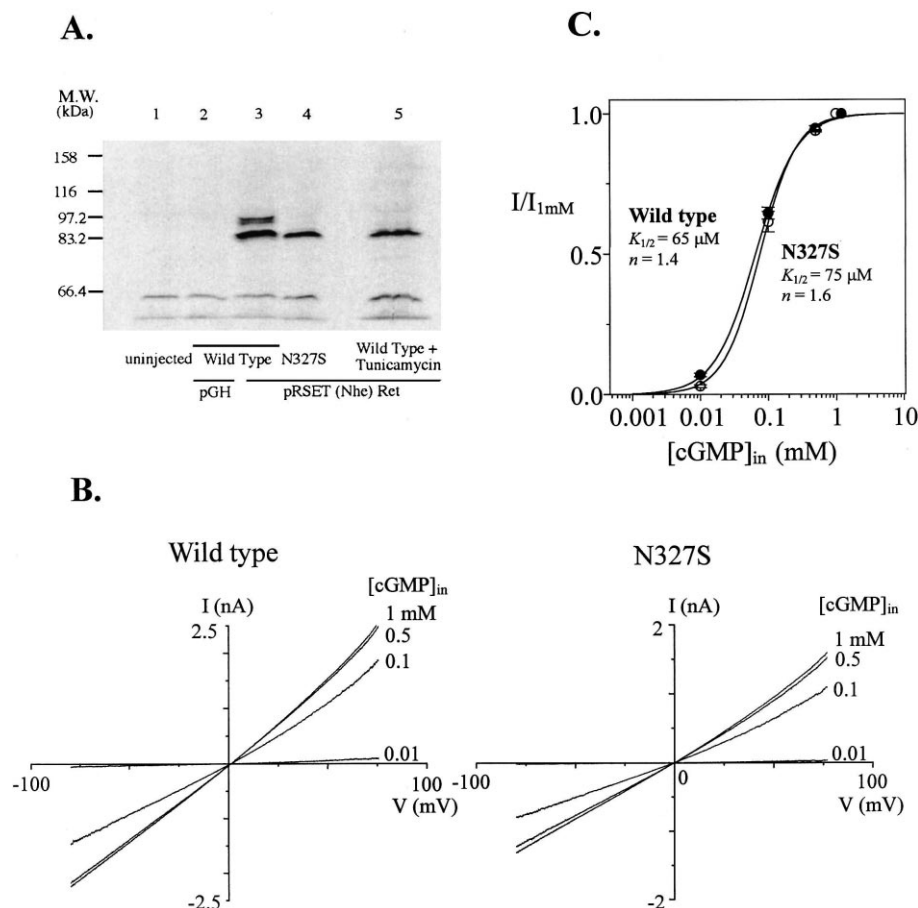
A.

C.

B.

Fig. 2. Effect of N327S mutation on the activation of channel currents by intracellular cGMP. A: In this immunoblotting experiment, total proteins of injected and uninjected oocytes were separated by SDS–PAGE and immunoblotted. Channel proteins were detected using anti T7-tag mouse antibody. (Lane 1: uninjected oocytes, lane 2: wild type without the T7-tag delivered in pGH vector, lane 3: wild type with the T7-tag in pRSET vector, Lane 4: N327S mutant with the T7-tag in pRSET, lane 5: Tunicamicin treated wild type with the T7-tag in pRSET). B: Macroscopic channel currents were recorded with inside-out membrane patches from the wild type and the N327S mutant mRNA injected oocytes at various concentrations of intracellular cGMP. C: The fraction of activated current (I) over fully activated current ($I_{1 \, mM}$) of the wild type (filled circles) and the N327S (empty circles) measured at 30 mV was plotted as a function of the intracellular cGMP concentration. The solid lines are fits of the data to the Hill equation, $I/I_{1 \, mM} = (1 + K_{1/2}^{n}/[cGMP]^{n})^{-1}$, with the activation constant $K_{1/2}$ and the Hill coefficient n.

3. Results

3.1. Biochemical analysis of bovine retinal CNG channel α subunit and N327S mutant expressed in Xenopus oocyte

All CNG channels including the bovine retinal CNG channel have one or more evolutionary conserved Asn–X–Ser/Thr motif between the S5 and the P-region (Fig. 1). The Asn-327 of the bovine retinal CNG channel α subunit was substituted with serine by site-directed mutagenesis to test the role of *N*-glycosylation at this site. Complementary RNAs of both wild type and N327S mutant channels were produced by in vitro transcription and were injected into *Xenopus* oocytes. Expressed channels were analyzed by immunoblot using anti-T7 monoclonal mouse antibody against the N-terminal T7-tag of the channel proteins (Fig. 2A).

When expressed in *Xenopus* oocyte, the wild type CNG channel showed a complex band pattern in SDS–PAGE and subsequent Western blot analysis. Although the molecular weight of unglycosylated bovine retinal CNG channel with T7-tag was calculated as 83 kDa, two other major bands were detected near 95 kDa besides the nascent 83 kDa band (Fig. 2A, lane 3). These high molecular weight protein bands

disappeared when the putative *N*-glycosylation site, Asn-327 residue, of this protein was replaced by a serine (N327S) (lane 4), or when the wild type channels were expressed in the presence of 10 μg/ml of tunicamycin, an inhibitor of *N*-acetylglucosaminase [22] (lane 5). The same effects caused by the treatment of tunicamycin and the mutation of the Asn-327 residue strongly suggested that the protein bands near 95 kDa are the glycosylated CNG channel proteins and the Asn-327 residue is the only site used for *N*-glycosylation. As a control, we used the protein sample from uninjected oocytes (lane 1) and the oocyte sample injected with the wild type CNG channel without T7-tag (lane 2).

3.2. N327S mutation does not affect the membrane expression level and the correct assembly of the CNG channel in Xenopus oocyte

The expression level of the functional channel was investigated directly by comparing their current level activated by intracellular cyclic GMP using patch clamp recording. There was no noticeable difference between the overall amplitudes of macroscopic current generated by injection of the same amount of mRNA from wild type and the N327S mutant
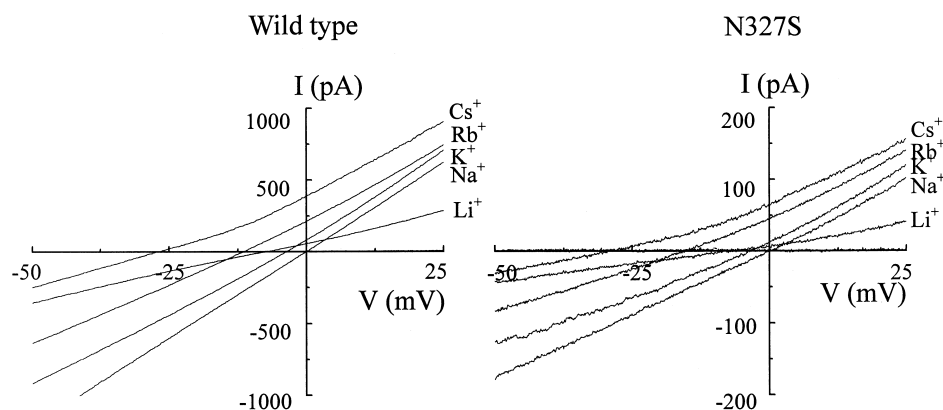
Fig. 3. Selectivity of the N327S mutant channel for monovalent cations. I–V relationships of the wild type and the N327S mutant channels were obtained under bi-ionic conditions. The pipette solution contained 130 mM NaOH, 3 mM HEPES, 0.5 mM EDTA (free acid form) adjusted to pH 7.6 with HCl. Perfusion solutions were identical to the pipette solution except the test ions (K^+, Li^+, Rb^+, or Cs^+) were substituted for Na^+. Cyclic GMP was added in intracellular solutions (pipette) to 500 μM for current activation.

channel (Fig. 2B). From 2 days after the microinjection of mRNA into *Xenopus* oocytes, the activation characteristics of both the wild type and the mutant channel by cGMP were investigated (Fig. 2C). Currents were normalized by the value at the saturation point of activation (1 mM cGMP) and fitted to the Hill equation (Fig. 2). The calculated half maximal activation constant ($K_{1/2}$) of the wild type and the N327S were not significantly different. Consequently, the gating characteristics of the wild type and N327 mutant channels were identical. This result suggests that de-glycosylation of the CNG channel does not affect the expression level and the functional assembly at the membrane of *Xenopus* oocytes.

3.3. Selectivity order for monovalent cations was slightly affected by N327S mutation

Under bi-ionic conditions, the reversal potentials of the wild type and the N327S mutant channel currents were measured for Na^+, K^+, Li^+, Rb^+ and Cs^+ ions against Na^+ ions at the opposite side (Fig. 3). From the four independent experiments, we obtained the reversal potential values of the wild type CNG channel and the N327S mutant channel under bi-ionic condition, as follows, in mV (wild type: Na^+, -0.17 ± 0.25; K^+, -3.70 ± 0.18; Li^+, -8.05 ± 0.39; Rb^+, -11.74 ± 0.64; Cs^+, -25.93 ± 0.90, N327S: Na^+, -0.17 ± 0.31; K^+, -3.99 ± 0.17; Li^+, -7.66 ± 0.53; Rb^+, -13.78 ± 0.55; Cs^+, -29.09 ± 0.34). After the compensation of the liquid junction potential, the selectivity order of the wild type channel among monovalent cations was determined as $Na^+ \sim K^+ > Rb^+ > Li^+ > Cs^+$ with a permeability ratio of 1:0.95:0.71:0.70:0.41, which was slightly different from the *N*-glycosylation mutant, $Na^+ \sim K^+ > Li^+ > Rb^+ > Cs^+$ with a ratio of 1:0.94:0.71:0.65:0.36.

3.4. Effects of the N-glycosylation mutation on the voltage-dependent blockade of the channel current by the intracellular or extracellular Mg^{2+}

The I–V relationships of the wild type and the N327S mutant channel measured in the presence of various concentrations of intracellular or extracellular Mg^{2+} are shown (Fig. 4A). Mg^{2+} blocks CNG channel in a voltage-dependent manner since the Mg^{2+} binding site is believed to lie within the transmembrane voltage drop [19]. As a permeant blocker, Mg^{2+} can permeate through the CNG channel at extreme

membrane voltages [19,20]. In the case of blockade by extracellular Mg^{2+}, the binding and the unbinding of Mg^{2+} to the binding site inside the pore is in near equilibrium without leaking through the pore in positive membrane voltages. However, in negative membrane voltages, the reaction deviates from the equilibrium. For intracellular Mg^{2+} blockade such deviations are observed in negative membrane voltages. Five independent data sets of titration were averaged, normalized and fitted to the Hill equation for both intra- and extracellular Mg^{2+}. The apparent half-blocking constant, K_i^{app} was calculated for each data set for both the wild type and the N327S mutant channel in the presence of extracellular and intracellular Mg^{2+}. The representative result calculated at 90 mV for extracellular and -30 mV for intracellular Mg^{2+} were shown for both the wild type and the N327S mutant (Fig. 4B). A slight difference in K_i^{app} values between the N327S mutant and the wild type was observed. Interestingly, this difference disappeared as the concentration of extracellular Mg^{2+} was increased from 10 to 100 mM. Intracellular Mg^{2+}, however, did not cause this phenomenon.

K_i^{app} values vary linearly with the membrane voltage in the equilibrium range and the slope can be used to calculate the electrical distances (δ) of the Mg^{2+} binding site on the membrane voltage drop from the extracellular side (Fig. 4C). Extracellular Mg^{2+} binding sites of the wild type and the mutant channel differ about 7% in terms of electrical distance. The difference is small in the case of intracellular Mg^{2+} block and Mg^{2+} seems to bind to almost the same position in both cases, about 88% of electrical distance from the extracellular side.

4. Discussion

To answer the question why an *N*-glycosylation site is so highly conserved throughout evolution of the CNG channel, we made a mutant channel to abolish the *N*-glycosylation and tested its effect. The wild type CNG expressed in *Xenopus* oocytes showed a complex pattern in denaturing gel electrophoresis. We detected not only the glycosylated high molecular weight bands but also a major protein band at the position of the unglycosylated channel near 83 kDa. Based on the previous studies of Shaker K^+ channel [23–27], we assumed that the protein band at 83 kDa is immature, and the ungly-
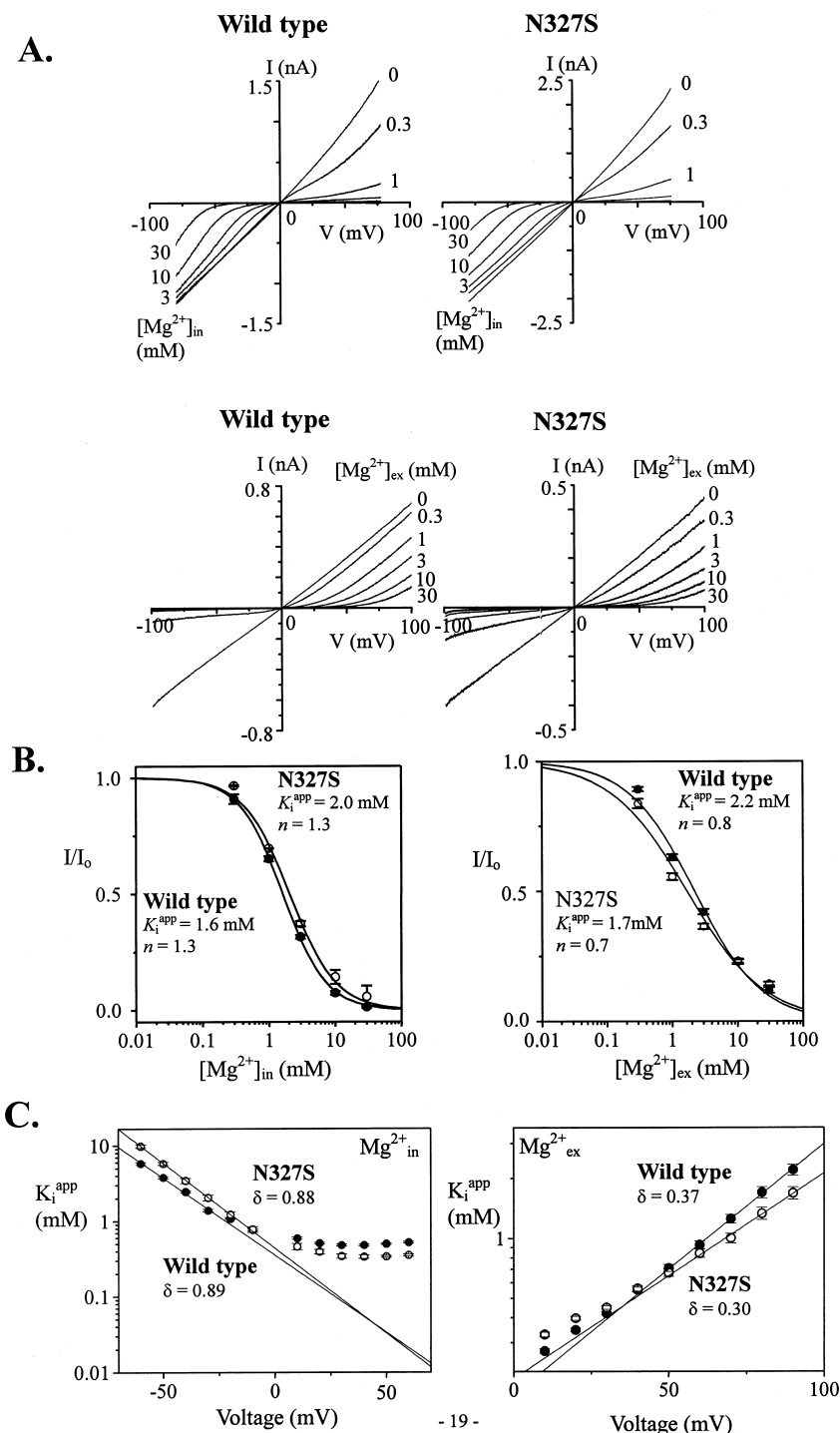
Fig. 4. Blockade of the wild type and the N327S mutant channel currents by Mg^{2+}. A: I–V relationships of the wild type (right panels) and the N327S mutant (left panels) channels in outside-out membrane patches blocked by intracellular (upper panels) or extracellular Mg^{2+} (lower panels) of various concentrations. B: The fraction of unblocked current (I/I_0) of the wild type (filled circles) and the N327S (empty circles) was plotted as the function of the intracellular (left panel) or extracellular Mg^{2+} (right panel) concentration. The solid lines are fits of the data to the Hill equation, $I/I_0 = (1+[Mg^{2+}]^n/K_i^{app\ n})^{-1}$, with the apparent blocking constant K_i^{app} and the Hill coefficient n. C: K_i^{app}'s for the intracellular (left panel) and extracellular (right panel) Mg^{2+} blockade of the wild type channel (filled circles) and the N327S mutant channel (empty circles) are plotted as a function of the membrane voltage. The solid lines are fits of the data to the equation $K_i^{app} = K_i^{app}(0\ mV) \times \exp(z\delta FV/RT)$. $K_i^{app}(0\ mV)$, concentrations in mM for the wild type and the mutant channel are as follows (extracellular Mg^{2+}: wild type, 0.17 mM; N327S, 0.20 mM. intracellular Mg^{2+}: wild type, 0.36 mM; N327S, 0.43 mM.)

cosylated channel protein is either waiting to be assembled or trapped in endoplasmic reticulum (ER). When expressed heterologously in *Xenopus* oocytes, Shaker protein is made as immature, core-glycosylated precursors in the ER where

they fold and assemble to tetramers. Upon transfer to the Golgi apparatus and processing of the oligosaccharide residues, the immature proteins are converted to the mature structure and delivered to cell membrane. In fact, the degree

of deglycosylation has been a useful indicator to assay those mutations in Shaker blocking channel maturation. In the case of N327S mutant channels, however, we only detected a single major protein band at 83 kDa. Since the unglycosylated channel proteins can not be separated from those trapped in ER electrophoretic techniques, we can not tell how much of this protein band is actually expressed on the cell surface. However, the complete disappearance of the higher molecular weight upon the mutation at Asn-327 or the treatment of N-glycosylation inhibitor indicates that the 'Asn–Asp–Thr' sequence in the extracellular linker between S5 and the P-region of CNG channel is truly utilized for N-glycosylation in vivo. Moreover, the same effects caused by the treatment of tunicamycin and the mutation strongly suggested that the Asn-327 of the CNG channel is the only site used for N-glycosylation. Since the abolition of N-glycosylation does not affect the expression and the correct assembly of the structure either, the general explanation about the role of the glycosylation of membrane proteins such as protein folding, sorting and membrane targeting seems not applicable to N-glycosylation of CNG channels.

It is also intriguing that this conserved N-glycosylation site is located in the outer vestibule of the channel near the P-region. Since the vestibules of ion channel are believed to influence the permeation of ions [18,28] and the P-region mainly determines the characteristics of permeation, glycosylation near the pore mouth can affect the channel function by the structural arrangement of the pore region and/or by surface charge effect as reported in the case of the sodium channel [12]. To investigate the permeation characteristics of the wild type and the N327S mutant, the bi-ionic experiment was performed to determine the selectivity. Another sensitive test of the alterations in the pore structure is to determine the characteristics of the Mg^{2+} blockade. The Glu-363 residue of the bovine retinal CNG channel is responsible for the blockade by external divalent cations and it forms the ring of selectivity filter by tetramerization. Small changes introduced by mutation or protonation on this residue are known to result in the alteration of the apparent affinity of the Mg^{2+} blockade [19,20,29].

Cyclic GMP-gated channels are non-selective cation channels permeating both Na^+ and K^+. These channels are also highly selective for divalent cations as permeant blockers [30,31]. Although, the similarity of amino acid residues known to form an ion-conducting pathway is high among CNG channels, their selectivity for monovalent cations can be different as revealed in the case of CNG channels of bovine rod and catfish olfactory neurons [32]. A recent molecular dynamics study suggests that strong electrostatic interactions with negatively charged residues in the outer vestibule cause ions located in the channel vestibule to lose part of their hydration shell and diffuse into the channel inner pore [18]. Thus, the different dehydration state of the conducting ions may be a determinant factor in the ion selectivity of the channel. The results from the bi-ionic experiments reveal that there is a change in the selectivity order between the wild type and the N327S mutant.

Investigating the extracellular and intracellular Mg^{2+} blockades can provide useful insights on the ionic permeation through the mutant channel. The apparent half-blocking constants (K_i^{app}) were determined for both extracellular and intracellular Mg^{2+}. Only K_i^{app} in the equilibrium range of the transmembrane voltage is meaningful in terms of affinity and has a linear relationship with voltage representing its voltage-dependent nature clearly. We found that small changes in K_i^{app} and its voltage dependent slope resulted from de-glycosylation. These changes can be explained as the surface charge contribution of glycosylation. Although the changes in the apparent affinity (K_i^{app}) of Mg^{2+} due to the de-glycosylation and their relationships with surface charge contribution and structural rearrangement cannot be interpreted in a straightforward manner, the surface charge effects of glycosylation may be responsible for the larger change occurring in the electrical distance of the external binding site than in that of the internal binding site [33]. Another evidence for the charge contribution by glycosylation is the charge screening effect by extracellular Mg^{2+} in the concentration of 10–100 mM, which is not observed in the identical concentration range of intracellular Mg^{2+}. Similar observations were also reported in the sodium channel [12].

In conclusion, the mutation of the well-conserved N-glycosylation in bovine retinal CNG channel affected the channel function by changing the electrostatic energy profile of the external vestibule near the pore. Although we assume that the unglycosylated wild type channel proteins are those trapped in ER, significant populations of the wild type channel proteins might be expressed at the cell surface without glycosylation, unlike other ion channels such as Shaker K^+ channels. Thus, the experimental results with the wild type channels can be explained by the heterogeneous populations of the glycosylated and unglycosylated forms. This would inevitably dilute the effects of the mutation and therefore, we would not be able to elucidate the physiological meaning of N-glycosylation. We also cannot exclude the general role of N-glycosylation such as protein targeting. CNG channels play important roles in sensory signal transduction and are localized in sensory organs [34]. Although the high-level of expression in Xenopus oocyte enables us to detect small structural and functional differences caused by glycosylation, it would be highly interesting to investigate the role of N-glycosylation for the localization of CNG channels in the membranes of polarized cells such as sensory receptor cells or neurons.

References

[1] Kaupp, U.B. (1991) Neuroscience 14, 150–157.
[2] Dryer, S.E. and Henderson, D. (1993) Nature 353, 756–758.
[3] Biel, M., Altenhofen, W., Hullin, R., Ludwig, J. and Freichel, M. (1993) FEBS Lett. 329, 134–138.
[4] Biel, M., Zong, X., Distler, M., Bosse, E. and Klugbauer, N. (1994) Proc. Natl. Acad. Sci. USA 91, 3505–3509.
[5] Bradely, J., Zhang, Y., Bakin, R. and Lester, H. (1997) J. Neurosci. 17, 1993–2005.
[6] Finn, J.T., Grunwald, M.E. and Yau, K.-W. (1996) Annu. Rev. Physiol. 58, 395–426.
[7] Bradely, J., Li, J., Davidson, N. and Lester, H. (1994) Proc. Natl. Acad. Sci. USA 91, 8890–8894.
[8] Liman, E. and Buck, L. (1994) Neuron 13, 611–621.
[9] Liu, D.T., Tibbs, G.R. and Siegelbaum, S.A. (1996) Neuron 16, 681–693.
[10] Kawamoto, S., Hattori, S., Sakimura, K., Mishina, M. and Okuda, K. (1995) J. Neurochem. 64, 1258–1266.

[11] Liu, Y., Eckstein-L., U., Fei, J. and Schwarz, W. (1998) Biochim. Biophys. Acta 1415, 246–254.

[12] Zhang, Y., Hartmann, H.A. and Satin, J. (1999) J. Membr. Biol. 171, 195–207.

[13] Schwalbe, R.A., Wang, Z., Wible, B.A. and Brown, A.M. (1995) J. Biol. Chem. 270 (25), 15536–15540.

[14] Bradshaw, R.A., McAlister-H., L. and Douglas, M.G. (1998) Molecular Biology of Intracellular Protein Sorting and Organelle Assembly, Alan R. Liss, New York.

[15] Matter, K. and Mellman, I. (1994) Curr. Opin. Cell Biol. 6, 545–554.

[16] Scheiffele, P., Peranen, J. and Simons, K. (1995) Nature 378, 96–98.

[17] West, C.M. (1986) Mol. Cell. Biochem. 72, 3–20.

[18] Guidoni, L., Torre, V. and Carloni, P. (1999) Biochemistry 38, 8599–8604.

[19] Root, M.J. and MacKinnon, R. (1993) Neuron 11, 459–466.

[20] Park, C.S. and MacKinnon, R. (1995) Biochemistry 34, 13328.

[21] Martell, A.E. and Smith, R.M. (1974) Critical Stability Constants, Vol. 1, pp. 204–271, Plenum Press, New York.

[22] Santacruz, T.L., Huang, Y., John, S.A. and Papazian, D.M. (1994) Biochemistry 33, 5607–5613.

[23] Nagaya, N. and Papazian, D.M. (1997) J. Biol. Chem. 272, 3022–3027.

[24] Papazian, D.M., Shao, X.M., Seoh, S.-A., Mock, A.F., Huang, Y. and Wainstock, D.H. (1995) Neuron 14, 1293–1301.

[25] Tiwari-Woodruff, S.K., Schulteis, C.T., Mock, A.F. and Papazian, D.M. (1997) Biophys. J. 72, 1489–1500.

[26] Schulteis, C.T., John, S.A., Huang, Y., Tang, C.-Y. and Papazian, D.M. (1995) Biochemsitry 34, 1725–1733.

[27] Schulteis, C.T., Nagaya, N. and Papazian, D.M. (1998) J. Biol. Chem. 273, 26210–26217.

[28] Hoyles, M., Kuyucak, S. and Chung, S.-H. (1996) Biophys. J. 70, 1628–1642.

[29] Rho, S.H. and Park, C.S. (1998) FEBS Lett. 440, 199–202.

[30] Yau, K.W. and Baylor, D.A. (1989) Annu. Rev. Neurosci. 12, 289–327.

[31] Capovilla, M., Caretta, A., Cervetto, L. and Torre, V. (1983) J. Physiol. 343, 295–310.

[32] Goulding, E.H., Tibbs, G.R., Liu, D. and Siegelbaum, S.A. (1993) Nature 364, 61–64.

[33] Hille, B. (1992) Ionic Channels of Excitable Membranes, 2nd Ed., Sinaur Associates, Inc., Sunderland, MA.

[34] Taylor, W.R. and Baylor, D.A. (1995) J. Physiol. 483, 567–582.